

# Retrospective evaluation of mandibular third molars using simulated low-dose cone-beam computed tomography: A comparative image quality study

Dalia Homar Asan<sup>1,\*</sup>, Josefine Cederhag<sup>1</sup>, Xie-Qi Shi<sup>2</sup>, Mats Nilsson<sup>1</sup>, Kristina Hellén-Halme<sup>1,2</sup>

<sup>1</sup>Department of Oral and Maxillofacial Radiology, Malmö University, Malmö, Sweden

<sup>2</sup>Section of Oral and Maxillofacial Radiology, Department of Clinical Dentistry, University of Bergen, Bergen, Norway

## ABSTRACT

**Purpose:** This study was performed to establish a procedure for simulated low-dose cone-beam computed tomography (CBCT) scans and to investigate whether the resulting images are comparable in diagnostic accuracy to those obtained using a clinical low-dose protocol.

**Materials and Methods:** ImageJ was used to manipulate the sinogram data from CBCT scans acquired at 5 mA to mimic a technical setting of 2 mA by adding noise to the Radon-transformed projection data before image reconstruction. Four observers compared the simulated 2 mA CBCT scans with original clinical 2 mA CBCT scans acquired previously. The CBCT images were analysed using a protocol with a ranking scale, and the observers were required to select only 1 category for each variable. The Wilcoxon signed-rank test was used to assess differences between the 2 CBCT scan types, with a significance level of  $P < 0.05$ . Intra-observer agreement was evaluated using the Cohen kappa.

**Results:** Pairwise observer comparisons of the simulated and clinical low-dose CBCT scans showed no significant differences in image quality. Intra-observer agreement was acceptable, and in 5 comparisons, the results indicated a high degree of agreement.

**Conclusion:** Simulated low-dose CBCT scans can be generated using ImageJ. No significant differences in image quality were observed between simulated and clinical low-dose CBCT scans when evaluating mandibular third molars. These findings suggest that manipulation of sinogram data is a promising radiation-free approach for simulating low-dose images in optimisation efforts. (*Imaging Sci Dent 20250212*)

**KEY WORDS:** Cone-Beam Computed Tomography, Image Quality, Radiation, Image Processing

## Introduction

For radiographic evaluations of structures in the oral cavity, cone-beam computed tomography (CBCT) provides information in 3 dimensions (the coronal, sagittal, and axial planes), unlike 2-dimensional (2D) intraoral imaging.<sup>1</sup> CBCT examinations are frequently used in a variety of dental contexts, most commonly for implant treatment planning and localisation of impacted teeth.<sup>2</sup> CBCT may be required when clinical examination and

conventional 2D radiography cannot provide adequate information to address the clinical question.<sup>3,4</sup> A previous study showed that 3D information can lead to different diagnoses and, consequently, different treatment plans compared with 2D radiography of the mandibular third molar.<sup>5</sup> However, CBCT examinations deliver higher radiation doses than 2D imaging.<sup>6</sup> Guidelines from the SEDENTEXCT consortium<sup>3</sup> concluded that CBCT should be used when conventional intraoral radiography does not provide adequate information. This applies, for example, when a mandibular third molar is to be removed and there is suspected close proximity between the mandibular canal and the tooth roots, but the relationship cannot be sufficiently evaluated with 2D radiography. Although CBCT provides high accuracy for the localisation and assess-

This study was supported by Malmö University, Sweden.  
Received August 7, 2025; Revised November 26, 2025; Accepted December 3, 2025  
Published online January 30, 2026

\*Correspondence to : Prof. Dalia Homar Asan  
Department of Oral and Maxillofacial Radiology, Faculty of Odontology, Malmö University, Carl Gustafs väg 34, 214 21 Malmö, Sweden  
Tel) +46-40-665-84-14, E-mail) dalia.homar-asan@mau.se

ment of anatomical features, the increased radiation dose must be considered.<sup>3</sup> The “as low as reasonably achievable” (ALARA) principle emphasises the importance of minimising the radiation dose and is applied in most countries worldwide. Improving radiation protection, including through optimisation of radiographic examinations, is therefore of great importance.<sup>7</sup> The “as low as diagnostically acceptable, indication-oriented, and patient-specific” (ALADAIP) principle builds on and extends ALARA, offering particular value in the optimisation of paediatric radiation exposure.<sup>8</sup>

Iskanderani et al.<sup>9</sup> reported that acceptable image quality for temporomandibular joint assessment could be maintained despite reducing tube current in CBCT imaging from 5 mA to 1 mA. Another study concluded that a 60% reduction in tube current provided acceptable image quality for pre-surgical assessment of the mandibular third molar in most cases.<sup>10</sup> Vicente et al. also confirmed the feasibility of reducing the radiation dose while maintaining diagnostically acceptable image quality.<sup>11</sup> These clinical studies aimed to determine whether low-dose CBCT protocols are sufficient for diagnostic evaluation, which is key to the optimisation process.

Prior research has theoretically verified that low-dose CBCT can be simulated (i.e., lower radiation exposure, reflected by a lower mAs value) by adding artificial noise to the raw projection data of standard-dose images.<sup>12</sup> Söderberg et al.<sup>12</sup> showed that the noise power spectrum (NPS; i.e., the noise texture) was similar between original and reconstructed images, and they concluded that the noise texture was reproduced correctly in the simulated radiography. Additionally, the findings indicated acceptable agreement in noise magnitude (<20% deviation in pixel standard deviation) between the original and simulated images. Båth et al.<sup>13</sup> investigated the possibility of simulating radiographic images representing a low radiation dose and concluded that their method was valid. Moreover, several studies have simulated radiographic images to analyse outcomes and found that these images can be used.<sup>14,15</sup> However, the question remains whether a CBCT examination can be simulated as a low-dose scan while maintaining diagnostically acceptable quality. It is therefore of considerable interest to investigate whether simulated low-dose CBCT images can be generated and whether their performance is comparable to that of clinically acquired low-dose images, thus evaluating the accuracy of the simulation. If the results are comparable to those obtained using a clinical low-dose protocol, this simulation may be used in future studies. Accordingly, the objectives of this study were to investigate

whether simulated low-dose CBCT scans could be generated and whether the images were comparable in diagnostic accuracy for the evaluation of mandibular third molars, compared with previously acquired scans obtained using a standard clinical protocol and a low-dose protocol. The hypothesis was that simulated low-dose CBCT scans would provide acceptable image quality, comparable to that of the original low-dose CBCT examination.

## Materials and Methods

### Study design

CBCT examinations of 60 mandibular third molars from a previous study by Cederhag et al.<sup>10</sup> were retrospectively collected for the present study. ImageJ (version 1.52n; National Institutes of Health, Bethesda, MD, USA, <http://rsb.info.nih.gov/ij/>) was used to simulate a low-dose protocol, manipulating scans acquired with an X-ray tube current of 5 mA to mimic a technical setting of 2 mA through addition of noise to the raw image data. These simulated 2 mA CBCT scans were compared with the original clinical 2 mA CBCT scans from the previous research.

### Ethical considerations

The scans of the 60 mandibular third molars were retrieved from a prior clinical study that had already been approved by the Swedish Ethical Review Authority and the Swedish Radiation Safety Authority.<sup>10</sup> The CBCT scans were anonymised; that is, no personal data could be retrieved. Therefore, according to Swedish law, no additional national ethical approval was required for the present study.

### CBCT examination

Two CBCT examinations of the region of interest (ROI), acquired using 2 different protocols, were used. One was obtained using a default standard clinical protocol (90 kV, 5 mA, 9.4 s) and the other with a low-dose protocol (90 kV, 2 mA, 9.4 s). The examinations were performed using a Veraviewepocs 3D F40 (J Morita Corp., Kyoto, Japan) with a field of view of 4.0 cm × 4.0 cm, a rotation mode of 180°, and a voxel size of 0.125 mm. The CBCT volumes were stored as Digital Imaging and Communications in Medicine files.

### Simulation of CBCT examination

In all types of computed tomography (CT), the acquired raw data projections are arranged using the Radon transform, introduced by the Austrian mathematician Johann

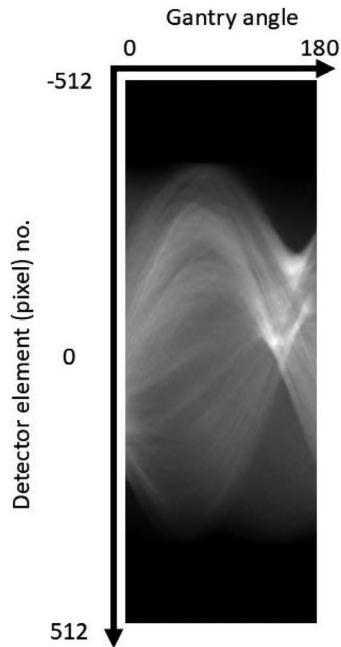


**Fig. 1.** Projection data of the Radon transform presented as a sinogram.

Radon in 1917. The Radon transform results in the projection data being stored in a 2D array called Radon space, or a sinogram, where the gantry angle is on the x-axis and the detector number (or detector pixel number) is on the y-axis (Fig. 1).

Before the projection data are reconstructed into the final image, they must be filtered by convolution with a kernel to avoid substantial artefacts. The choice of kernel depends on the clinical question at hand. Use of the kernel shown in Fig. 2 results in an image with good low-contrast resolution, poor spatial resolution, and low noise. Use of the kernel presented in Fig. 3 produces an image with poor low-contrast resolution, good spatial resolution, and high noise.

As the authors lacked access to the object's raw projection data, the 5 mA image was used as input to the Radon transform. The resulting sinogram is very similar to that of the object, but it also contains the data resulting from convolution with the filter (kernel) selected by the CBCT operator. Repeating the convolution with a sharper kernel introduces noise into the sinogram and, after application of an inverse Radon transform (back-projection), produces an image with a noise level and NPS close to that of the true 2 mA image. The procedure is illustrated in Fig. 4. The scan was stored as an AVI file. Simulation and interpretation of the CBCT examination were performed using ImageJ.

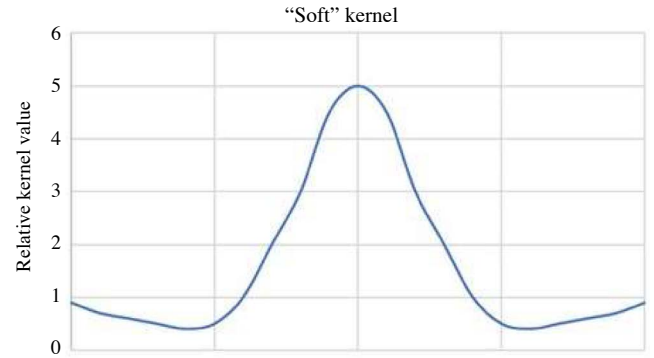


**Fig. 2.** Kernel values that produce an image with good low-contrast resolution, poor spatial resolution, and low noise.

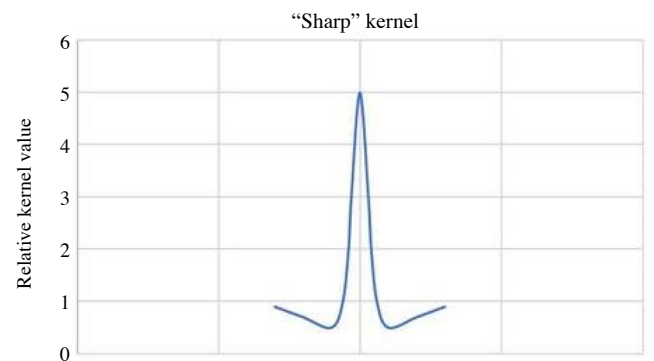


**Fig. 3.** Kernel values that produce an image with poor low-contrast resolution, good spatial resolution, and high noise.

### Choosing the appropriate kernel

Standard deviation is not a complete description of image noise, as it provides no information about the spatial characteristics (texture) of the noise. The magnitude of the NPS reflects the degree of randomness at each spatial frequency, while its shape indicates where the noise power is concentrated in frequency space. The NPS can be defined<sup>16</sup> as follows:

$$\text{NPS}(u,v) = N_x N_y \Delta_x \Delta_y \langle |\text{FT}\{\Delta I(x,y)\}|^2 \rangle \quad (1)$$

where  $\Delta I$  is the deviation from the mean of a noise image;  $N_x$  and  $N_y$  are the number of pixels; and  $\Delta_x$  and  $\Delta_y$  are the pixel sizes in the x- and y-directions, respectively. FT refers to the Fourier transform of the pixel deviations from the mean. However, for the sole purpose of comparing spectra across different images, a relative NPS can be used, and the expression can be simplified to:

$$\text{NPS}_{\text{rel}}(x,y) = \langle |\text{FT}\{P(x,y)\}|^2 \rangle \quad (2)$$

where  $P(x,y)$  represents the pixel values. This simplifi-

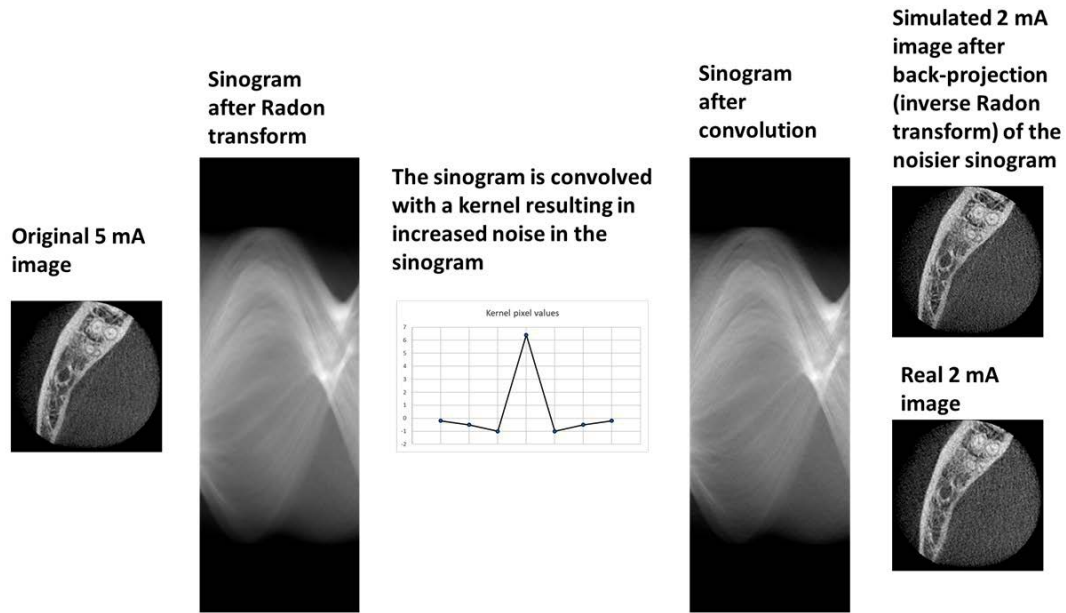


**Fig. 4.** Visual summary demonstrating the procedure for introducing noise into the sinogram and producing a simulated low-dose cone-beam computed tomography image.



**Fig. 5.** Example of a region of interest drawn in soft tissue regions.

cation follows from the fact that  $N_x \cdot N_y \cdot \Delta_x \cdot \Delta_y$  is a constant, and using  $P(x,y)$  instead of  $\Delta I(x,y)$  simply adds an offset. In the following procedure, this relative NPS is used. A  $128 \times 128$  pixel ROI was drawn (Fig. 5) in soft tissue regions of images acquired at 5 mA, 2 mA, and simulated 2 mA. The Fourier transform of a 2D image is also a 2D image, with spatial frequency on the x-axis

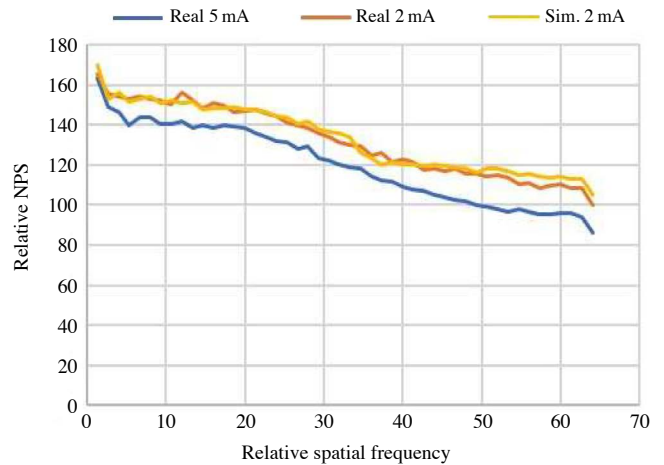


**Fig. 6.** Noise power spectra (NPS) for the region of interest (in Fig. 5) for 5 mA, 2 mA and simulated 2 mA, respectively.

is and phase angle on the y-axis. Commonly, the NPS is presented as a 1D curve integrated over all phase angles. Relative 1D NPS curves were calculated using the Radial Profile Plot plug-in in the image processing program ImageJ. For each image, the Fourier transform of the ROI was computed and, using the plug-in, profile plots of normalised integrated intensities around concentric circles were generated as a function of distance from the centre of the Fourier-transformed image. The intensity at a given distance from the centre represents the sum of pixel values around a circle (i.e., for a certain phase angle) with

**Table 1.** Examination protocol of anatomical variables

Anatomical variables	Categories
Relationship (MC and #8 mesial root)	Buccal <sup>a</sup> Lingual <sup>b</sup> Inferior <sup>c</sup> Inter-radicular if root appears bifid Not assessable
Proximity (between MC and #8 mesial root)	More than 1 mm Direct contact, with continuity of MC Direct contact, with discontinuity of MC (deformed canal)
Periodontal ligament (all roots)	Visible periodontal ligament Partially visible periodontal ligament Periodontal ligament not visible
Root morphology (all roots)	Convergent, Straight root/s Divergent, Claw-shaped, Convergent with curved root/s in the direction and towards path of elevation Atypical, Root dilaceration, Root/s either curved in opposite direction or against path of elevation
Root resorption of second molar (extended at least to outer half of dentine)	Yes Uncertain No

MC: mandibular canal. a: MC located straight buccally in relation to the root. b: MC located straight lingually in relation to the root. c: MC located inferiorly, either straight below or in the lingual/buccal direction.

**Table 2.** Pairwise comparisons of simulated low-dose versus clinical low-dose protocol for image variables among observers (*P*-values determined by Wilcoxon signed-rank test)

Image variables	Observer 1	Observer 2	Observer 3	Observer 4
Relationship	1.000	0.665	0.146	0.655
Proximity	0.225	<0.05	0.430	<0.05
Periodontal ligament	0.248	0.841	0.549	<0.05
Root morphology	<0.05	0.248	1.000	<0.05
Root resorption	0.608	0.180	0.083	<0.05
Subjective image quality	0.216	0.071	0.448	0.414

that distance as its radius. The integrated intensity was divided by the number of pixels in the circle to yield normalised values. The profile x-axis was plotted as relative spatial frequency (Fig. 6).

The procedure was repeated for 10 randomly selected images using several kernels to convolve the sinogram data, and the kernel that, on average, produced NPS data closest to that of the true 2 mA image was selected for processing the entire image dataset.

### Image evaluation

All observers were blinded to the examination protocol, and the CBCT examinations were randomly coded before interpretation. Four oral and maxillofacial radiologists

were calibrated using the protocol applied for assessment of the CBCT examinations. Three were senior oral and maxillofacial radiologists, and 1 was a resident in oral and maxillofacial radiology. The evaluations were performed individually, and the interpretation procedure incorporated all 3 planes of the image stack. Approximately 1 month later, all observers re-evaluated 10 randomly selected cases to determine intra-observer agreement. The images were analysed using the same settings as in the initial evaluation. In summary, the variables assessed were the relationship and proximity between the third molar and the mandibular canal, the periodontal ligament and root morphology of the third molar, root resorption of the second molar, and subjective image quality. The categories for each variable were

described in a previous study by Cederhag et al.<sup>10</sup> and are presented in Table 1. Observers were permitted to select only 1 category for each variable.

### Statistical analysis

A previous study by Cederhag et al.<sup>10</sup> reported a power analysis indicating that a minimum of 60 third molars was required to achieve a power of 0.8 at a significance level of  $P < 0.05$ . The present study compared image-variable results pairwise for each observer, specifically regarding the simulated low-dose protocol versus the clinically acquired low-dose protocol. Differences between these protocols were assessed using the Wilcoxon signed-rank test, with  $P$ -values of less than 0.05 considered to indicate statistical significance. Cohen weighted kappa values were calculated to quantify the intra-observer agreement, while the Fleiss kappa was used to determine inter-observer agreement according to the Landis and Koch scale.<sup>17</sup> SPSS version 28 for Windows (IBM Corp., Armonk, NY, USA) was used for data analysis.

## Results

Pairwise observer comparisons between simulated and clinical low-dose protocols showed no significant differences in assessment of the relationship between the mesial root of the third molar and the mandibular canal, or in overall image quality. For 3 observers, significant differences

were similarly absent for the periodontal ligament and for root resorption. For the proximity and root morphology variables, the responses of 2 observers yielded no significant differences. Observers 1 and 2 each showed 1 statistically significant difference among the image variables. Observer 4 displayed statistically significant differences in 4 of the 6 image variables, whereas observer 3 showed none (Table 2).

Most  $\kappa$  values for inter-observer agreement were in the moderate range (Table 3). Overall subjective image quality, visibility of the periodontal ligament, and root morphology had the lowest  $\kappa$  values and were categorised as fair agreement. Relationship, proximity, and root resorption displayed the highest  $\kappa$  values (Table 3). Table 4 shows acceptable intra-observer agreement. In 5 instances,  $\kappa$  values could not be calculated because the ratings displayed no variability, indicating complete agreement in those cases.

## Discussion

Several studies have investigated outcomes when simulating radiographic examinations. However, these have used various techniques and evaluated different anatomical regions.<sup>14,15,18,19</sup>

Kim et al.<sup>15</sup> evaluated the image quality of artificial intelligence (AI) processed low-dose CBCT. They transformed low-dose CT images into images with reduced noise, with spatial resolution adjusted by kernel modification. Their results showed acceptable agreement between the AI-processed low-dose CBCT and the standard-protocol CBCT group. However, the study design by Kim et al.<sup>15</sup> differed from the present research. In this study, noise was added to standard-protocol CBCT images by modifying the sinogram kernel, which is a theoretically verified approach described by Söderberg et al.<sup>12</sup>

The present study showed no significant difference between clinical low-dose and simulated images in assessment of the relationship between the mesial root of the mandibular third molar and the mandibular canal across

**Table 3.** Inter-observer agreement (Fleiss kappa)

Image variable	Low-dose protocol	Simulated-dose protocol
Relationship	0.596	0.578
Proximity	0.522	0.402
Periodontal ligament	0.220	0.299
Root morphology	0.393	0.247
Root resorption	0.684	0.532
Subjective image quality	0.130	0.253

**Table 4.** Intra-observer agreement (Cohen kappa)

Image variables	Observer 1	Observer 2	Observer 3	Observer 4
Relationship	0.928	1.000	1.000	0.713
Proximity	0.909	0.769	0.727	0.796
Periodontal ligament	–	0.706	0.412	0.737
Root morphology	0.561	0.800	0.643	0.884
Root resorption	–	0.000	–	–
Subjective image quality	0.000	0.000	1.000	–

observers. This is clinically useful, as accurate evaluation of these structures is essential when considering surgical removal of a third molar. Furthermore, none of the observers' responses yielded significant differences in overall image quality between the 2 imaging modalities. For 3 observers, periodontal ligament visibility and root resorption also did not differ significantly. For most comparisons, no significant differences were found between the simulated images and the clinical low-dose protocol. However, 1 observer's responses produced significant differences for several variables. Further analysis suggested that these differences often occurred between similar categories and may reflect intra-observer variation. Alternatively, the assessment guidelines may not have been sufficiently precise, possibly contributing to the observed differences (Table 2).

The present study found no significant difference between the simulated and clinical low-dose protocols in terms of subjective image quality. This contrasts with the study by Cederhag et al.,<sup>10</sup> in which the scores of 2 observers yielded a significant difference in subjective image quality between default and low-dose protocols.<sup>10</sup> Furthermore, in the present study, only 1 observer showed a significant difference when assessing the periodontal ligament, compared with the previous study in which 3 observers did so. These findings suggest that the image quality of the simulated low-dose CBCT stack was comparable to that of the clinical low-dose protocol.

The comparison of this study to other research in the literature is limited by variations in study design. Frush et al.<sup>18</sup> used a simulation technique to evaluate radiation dose reduction by adding a random Gaussian noise distribution to a CT scan after validating the method using a water phantom.<sup>18</sup> Ladefoged et al.<sup>19</sup> used a deep learning (DL) tool for noise reduction in low-dose positron emission tomography (PET) images to investigate whether image quality could support more accurate diagnostic reliability. LMChopper (e7-tools; Siemens Healthineers, Knoxville, TN, USA) was applied to reduced-dose PET raw data to reconstruct PET images with less noise. The authors concluded that with their DL model, a significant dose reduction could be achieved while maintaining diagnostically acceptable image quality.<sup>19</sup>

One limitation of this study was the inherent subjectivity of observer assessments. Another was the time-consuming nature of the manual procedure, with simulation results influenced by the individual performing the task. This limitation may be addressed in the near future through the use of AI.

In keeping with the ALARA and ALADAIP principles, there is an ongoing need to optimise radiation doses. Studies requiring multiple X-ray examinations in humans may face ethical concerns.<sup>10</sup> The development of ethically acceptable optimisation methods is therefore important in radiation protection. Because optimisation is device-specific, it is rarely possible to develop general recommendations for precise exposure parameter settings. However, the present study indicates that, by manipulating sinogram data, it is possible to generate a low-dose CBCT stack from a default CBCT stack in ImageJ. This approach could be used in future research to simplify optimisation efforts and facilitate implementation in other radiological practices. In conclusion, simulated low-dose CBCT scans can be generated, and no significant differences in image quality were observed compared with clinically acquired low-dose CBCT scans. These findings suggest that manipulation of sinogram data is a promising radiation-free method for simulating low-dose images in optimisation efforts.

**Conflicts of Interest:** None

## Acknowledgments

Dr. Karin Näsström participated in image evaluation and is therefore acknowledged by the authors.

## References

1. Scarfe W, Farman A, Sukovic P. Clinical applications of cone-beam computed tomography in dental practice. *J Can Dent Assoc* 2006; 72: 75-80.
2. Hol C, Hellén-Halme K, Torgersen G, Nilsson M, Møystad A. How do dentists use CBCT in dental clinics? A Norwegian nationwide survey. *Acta Odontol Scand* 2015; 73: 195-201.
3. European Commission. Radiation protection No 172. Cone beam CT for dental and maxillofacial radiology. Evidence based guidelines [Internet]. Luxembourg: Publications Office of the European Union; 2012 [cited 2024 Sep 27]. Available from: [https://sedentext.eu/files/radiation\\_protection\\_172.pdf](https://sedentext.eu/files/radiation_protection_172.pdf).
4. Kapila S, Nervina J. CBCT in orthodontics: assessment of treatment outcomes and indications for its use. *Dentomaxillofac Radiol* 2015; 44: 20140282.
5. Haney E, Gansky SA, Lee JS, Johnson E, Maki K, Miller AJ, et al. Comparative analysis of traditional radiographs and cone-beam computed tomography volumetric images in the diagnosis and treatment planning of maxillary impacted canines. *Am J Orthod Dentofacial Orthop* 2010; 137: 590-7.
6. Ludlow JB, Davies-Ludlow LE, Brooks SL. Dosimetry of two extraoral direct digital imaging devices: NewTom cone beam CT and Orthophos Plus DS panoramic unit. *Dentomaxillofac Radiol* 2003; 32: 229-34.

7. The 2007 Recommendations of the International Commission on Radiological Protection. ICRP publication 103. *Ann ICRP* 2007; 37: 1-332.
8. Oenning AC, Jacobs R, Pauwels R, Stratis A, Hedesiu M, Salmon B, et al. Cone-beam CT in paediatric dentistry: DIMITRA project position statement. *Pediatr Radiol* 2018; 48: 308-16.
9. Iskanderani D, Nilsson M, Alstergren P, Shi XQ, Hellén-Halme K. Evaluation of a low-dose protocol for cone beam computed tomography of the temporomandibular joint. *Dentomaxillofac Radiol* 2020; 49: 20190495.
10. Cederhag J, Iskanderani D, Alstergren P, Shi XQ, Hellén-Halme K. Visibility of anatomical landmarks in the region of the mandibular third molar, a comparison between a low-dose and default protocol of CBCT. *Acta Odontol Scand* 2023; 81: 449-55.
11. Vicente A, Cederhag J, Rashidi N, Wiedel AP, Becker M, Brogårdh-Roth S, et al. Low-dose cone-beam computed tomography in Swedish pediatric patients with alveolar clefts following alveolar bone grafting—a clinical study. *Clin Exp Dent Res* 2024; 10: e70021.
12. Söderberg M, Gunnarsson M, Nilsson M. Simulated dose reduction by adding artificial noise to measured raw data: a validation study. *Radiat Prot Dosimetry* 2010; 139: 71-7.
13. Båth M, Håkansson M, Tingberg A, Månsson LG. Method of simulating dose reduction for digital radiographic systems. *Radiat Prot Dosimetry* 2005; 114: 253-9.
14. Veldkamp WJ, Kroft LJ, van Delft JP, Geleijns J. A technique for simulating the effect of dose reduction on image quality in digital chest radiography. *J Digit Imaging* 2009; 22: 114-25.
15. Kim NH, Yang BE, Kang SH, Kim YH, Na JY, Kim JE, et al. Preclinical and preliminary evaluation of perceived image quality of AI-processed low-dose CBCT analysis of a single tooth. *Bioengineering (Basel)* 2024; 11: 576.
16. Dobbins JT. III. Image quality metrics for digital systems. In: Beutel J, Knudde HL, Van Metter RL. *Handbook of medical imaging. Vol. I. Physics and psychophysics*. Bellingham: SPIE Optical Engineering Press; 2000. p. 161-222.
17. Landis JR, Koch GG. The measurement of observer agreement for categorical data. *Biometrics*. 1977; 33: 159-74.
18. Frush DP, Slack CC, Hollingsworth CL, Bisset GS, Donnelly LF, Hsieh J, et al. Computer-simulated radiation dose reduction for abdominal multidetector CT of pediatric patients. *AJR Am J Roentgenol* 2002; 179: 1107-13.
19. Ladefoged CN, Hasbak P, Hornnes C, Højgaard L, Andersen FL. Low-dose PET image noise reduction using deep learning: application to cardiac viability FDG imaging in patients with ischemic heart disease. *Phys Med Biol* 2021; 66: 054003.